



Substantial Impact of Precipitants and Dispersant on the Structural and Optical Properties of CeO_2 Nanoparticles

R. Suresh ^{a,*}, K. Thirumal Valavan ^a, M. Justin Paul ^a, T. Indira Priyadharshini ^a

^a Department of Physics, Sri Ramakrishna Mission Vidyalaya College of Arts and Science, Coimbatore - 641 020, Tamil Nadu, India.

* Corresponding Author: rsdphy@gmail.com

Received: 30-07-2021, Revised: 28-09-2021, Accepted: 01-10-2021, Published: 30-10-2021

Abstract: Cerium oxide nanoparticles are prepared by simple precipitation method with various precipitants. The prepared samples are analyzed by XRD, FT-IR and PL. XRD confirms the occurrence of single-phase polycrystalline cubic fluorite structure with dominant orientation along (111) direction. The sharp band at 1415 cm^{-1} originated from $-\text{CH}_3$ deformation and $-\text{CH}_2$ scissoring vibrations of PVP, also A strong band at 848 and 400 cm^{-1} due to the envelope of the phonon band of the metal oxide (Ce-O) network obtained from FT-IR spectra. PL spectra exhibit the presence of strong blue and weak blue-green emission in the visible region. Additions of PVP strongly distress the peaks intensity of the samples.

Keywords: CeO_2 , PVP, FT-IR, KOH, NaOH

Introduction

With the increasing global demand for low cost solar cells are being scalable to high power level, transition metal oxides (TMO) semiconductors started to be considered as a promising material for such applications [1]. The majority of TMOs are abundant raw materials, non-toxic, low cost, simple manufacturing process and chemically stable, which enable material production under atmospheric conditions [2]. In particular, the combination of rare earth (RE) elements with wide band-gap semiconductors has stimulated a lot of attention and renowned many achievements in the technologies of catalysis, sensors, sun-screen materials, electrochemical devices, optoelectronics devices and polishing materials [3-6]. As one of the most important rare-earth oxides, CeO_2 is an attractive material for many technologies and has been widely used for diverse fields.

Among the pervasive preparation methods, the homogeneous precipitation method has received much attention due to its inherent advantages like simple, low cost and highly consistent process without introducing impurity elements to prepare nanoparticles. To the best of our

knowledge, only few authors report the photovoltaic properties of cerium oxide nanoparticles [7, 8]. An attempt has been made to synthesize rare earth materials like cerium oxide nanoparticles.

Experimental Details

Cerium oxide nanoparticles are prepared by precipitation method as reported in elsewhere [9]. Cerium oxide nanoparticles are prepared using cerium nitrate, aqueous ammonia, potassium hydroxide, sodium hydroxide and PVP purchased from HIMEDIA, Mumbai and used without further purification. For the synthesis, 0.1 M of cerium nitrate hexahydrate ($\text{Ce}(\text{NO}_3)_6 \cdot 6\text{H}_2\text{O}$) is dissolved in 50 ml of de-ionized water and strongly stirred for 30 min, then 25 ml of aqueous ammonia (NH_3) solution is added drop-wise to the above solution for 20 min and persistently stirred for 12h at room temperature. Interesting color changes appeared in the solution when precipitant (NH_3) was added to cerium nitrate solution. Initially at low pH, the light brown slurry formed due to Ce^{3+} , which is turned into light white-black color in 2 hours and turned into brown color after 3 hours, then light orange after 5 hours. Finally, at the end of the reaction, the slurry formed is light yellow in color due to the Ce^{4+} formation with the addition of oxygen. The obtained slurry is filtered and washed several times with de-ionized water and ethanol. The washed precipitate is dried in an oven at 60°C for 5h. The same experimental procedure is followed to prepare the samples with different precipitating agents potassium hydroxide (KOH) and sodium hydroxide (NaOH). The PVP is also added to the above precursor solutions to observe the morphological changes.

Result and Discussion

Structural properties

Figure 1 shows the XRD pattern of the cerium oxide nanoparticles prepared with different precipitating agents. The diffraction peaks correspond to (111), (200), (220), (311) and (400) planes of face centered cubic fluorite structure which fits with standard JCPDS (34-0394). There is no evidence for crystalline Ce_2O_3 phase is not detected in the XRD pattern, so it indicated the single-phase polycrystalline structure. Diffraction lines are very broad, indicating smaller crystallite size calculated using the Scherer's equation. The calculated crystallite size is found to be in the range 5.9-19.1 nm. The various structural parameters are calculated and listed in Table 1. The variation in the lattice parameter is attributed to the lattice strain induced by the introduction of Ce^{3+} due to arise of oxygen vacancies [10]. Therefore, it concluded that the decrease of crystallite size resulted in the increase of Ce^{3+} content, lattice strain and lattice parameter as evidenced from Table 1. The dispersant PVP strongly distorts the structural parameters of the samples prepared from NH_3 precipitant whereas slightly distorts the same prepared from NaOH and KOH precipitants.

Figure 2 shows the FT-IR spectra of CeO_2 nanoparticles prepared with different precipitating agents (NH_3 , NaOH and KOH).

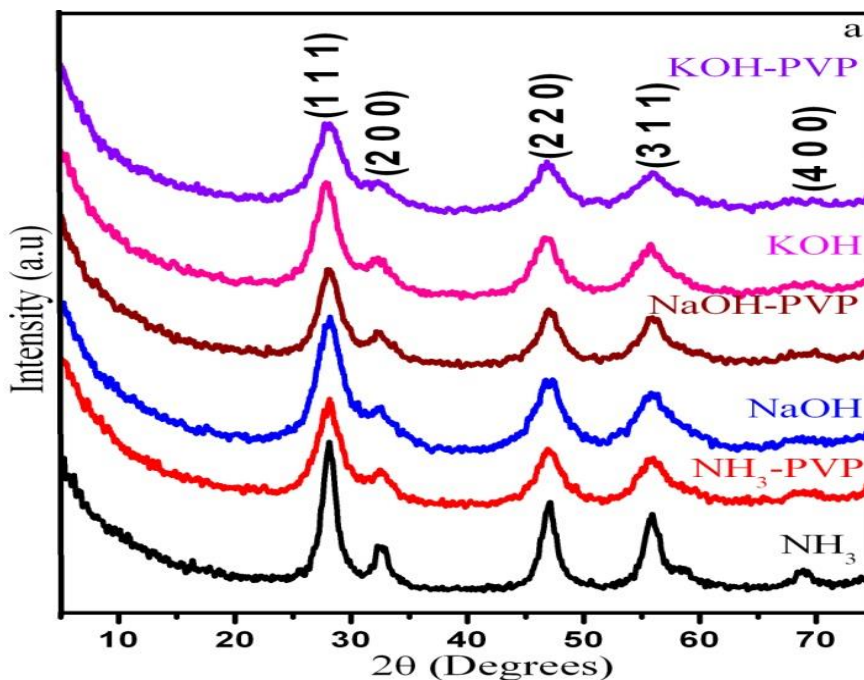


Figure 1 XRD pattern of cerium oxide nanoparticles

It reveals that the group of strong intense bands are observed at 3417, 1506 and below 700 cm^{-1} , weak bands are observed at 2926-2851, 1744, 1629, 1415, 1341, 1170-1000 and 848 cm^{-1} respectively. The observed bands can be assigned as follows: The intense bands at 3417 and 1629 cm^{-1} assigned to the O-H stretching and H-O-H bending modes of vibrations, respectively and indicate the presence of water molecules due to the moisture adsorbed from the atmosphere. Residual water and hydroxyl groups are usually observed in as-prepared samples and can be eliminated during heat treatment [11]. A group of weak intensity bands centred at 2926 and 2851 cm^{-1} are assigned to $\gamma(\text{C-H})$ mode of organic moieties and $\gamma(\text{CH}_2)$ respectively. The sharp band at 1415 cm^{-1} originated from $-\text{CH}_3$ deformation and $-\text{CH}_2$ scissoring vibrations of PVP. Additional bands observed at 1744, 1341 and 1170-1000 cm^{-1} are most probably associated to the presence of C=O stretching, COO^- stretching and C-O stretching modes of carbonate species on the ceria surface respectively. It has been advocating that carbon dioxide is predictable adsorbent on ceria surfaces at RT and is indicative of high surface basicity of surface O^{2-} ions for ceria. This specifies the surface carbonate species play an essential role in the preservation of surface area and porosity of the prepared material. There is no clear evidence of cerium nitrate (1380 cm^{-1}) present in the precursor due to the overlapping of peaks [12]. A strong band at 848 and around 400 cm^{-1} which is due to the envelope of the phonon band of the metal oxide (Ce-O) network [13].

Table 1. Structural parameters of cerium oxide nanoparticles

Sample name	2 Theta	FWHM	hkl	Crystallite Size (nm)	Texture Coefficient	Lattice Constant (nm)
NH ₃	28.0853	0.6298	111	13.5	0.92955	5.5031
	32.4167	0.9446	200	19.1	0.79043	5.5238
	47.1094	0.6298	220	14.3	1.05290	5.4564
	55.9404	0.7872	311	11.9	1.07562	5.4517
	68.9390	1.1520	400	18.7	1.15148	5.4441
NH ₃ -PVP	28.2762	1.4377	111	5.9	0.87531	5.4667
	32.5346	0.3100	200	7.8	1.03520	5.5043
	46.9649	1.3692	220	6.6	0.90037	5.4722
	56.0990	0.4284	311	7.9	0.78278	5.5225
	69.2310	0.3072	400	6.8	1.40597	5.4584
NaOH	28.28	0.7564	111	11.3	1.03916	5.4660
	32.9256	0.1628	200	13.8	0.96469	5.4711
	47.0669	0.3846	220	12.1	1.06114	5.4611
	56.0578	0.1123	311	13.6	0.93500	5.4411
NaOH-PVP	27.9975	0.4840	111	7.6	1.00968	5.5200
	32.5800	0.4425	200	9.5	0.87203	5.4969
	46.9737	0.3897	220	9.2	1.11725	5.4713
	55.7900	0.3000	311	8.9	1.00103	5.4570
KOH	28.2340	0.0909	111	13.5	1.09588	5.4747
	32.3000	0.5307	200	12.2	0.80474	5.5432
	46.9609	0.2782	220	12.5	1.04783	5.4727
	55.9522	0.3634	311	15.8	1.05153	5.4506
KOH-PVP	27.7700	0.5610	111	10.2	1.00779	5.5643
	32.4500	0.6154	200	11.0	1.11025	5.5183
	46.9957	0.7181	220	10.5	0.94422	5.4689
	56.0679	0.1988	311	10.8	0.93772	5.4402

Assimilation of PVP strongly increases the transmittance of the samples prepared from KOH precipitant, whereas moderately increases the same prepared from NaOH precipitant but slightly increases the same prepared from NH_3 precipitant. It also firmly affects the growth of O-H, H-O-H and carbonate bands (C=O and COO) whereas slightly affects the growth of C-O stretching vibrations as shown in Figure 2.

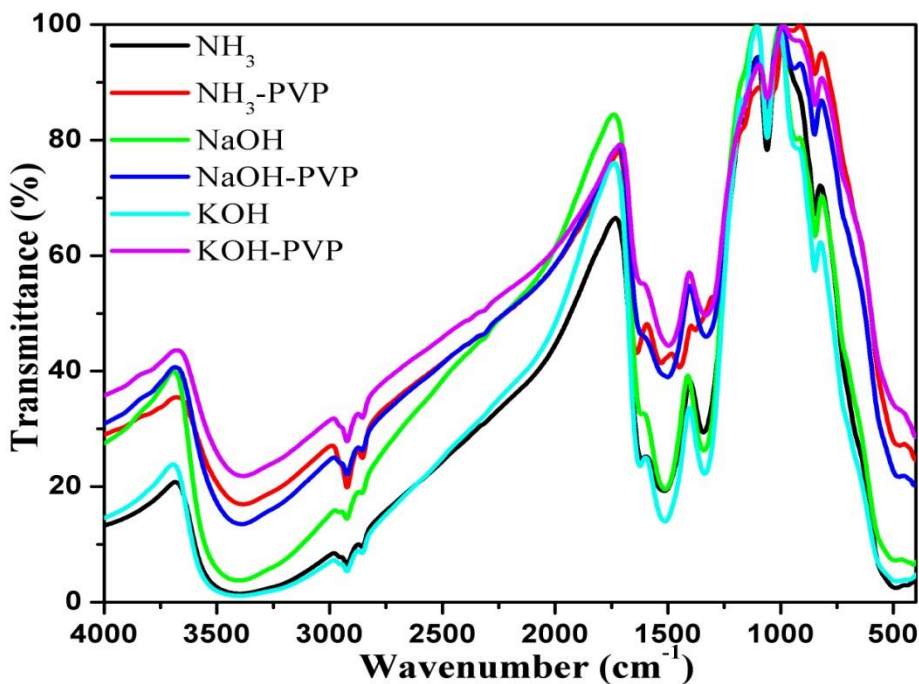


Figure 2. FT-IR spectra of cerium oxide nanoparticles

Optical Properties

Figure 3 shows the room temperature PL spectra of CeO_2 nanoaggregates obtained using Xenon laser of 325 nm as the excitation source. It consist of strong and sharp blue emission band at 425 nm (2.96 eV) and two low intensity peaks at 366 nm (3.39 eV) in the UV region and weak and broad blue-green emission band at 466 nm (2.66 eV) in the visible region. It suggested that the weak emission peak observed at 366 nm related to the trapping of electrons from defects level to $\text{O } 2p$ level [14]. It revealed that the strong and sharp blue emission peak observed at 425 nm due to the charge transitions between 4f band and valance band ($\text{O } 2p$) in CeO_2 . The defects energy levels between Ce 4f and O 2p are dependent on the temperature and density of defects in the crystal. It also cleared that the weak and broad blue-green emission peak at 466 nm is possibly due to low-density oxygen vacancies incorporated in the sample [15]. Incorporation of PVP strongly reduces the peaks intensity of the samples prepared from NH_3 precipitant, whereas moderately reduces the same prepared from NaOH precipitant but slightly reduces the same prepared from KOH precipitant due to the chemical inertness of the

precipitants as shown in Figure 3. The samples prepared from ammonia precipitant shows higher PL intensity than other samples.

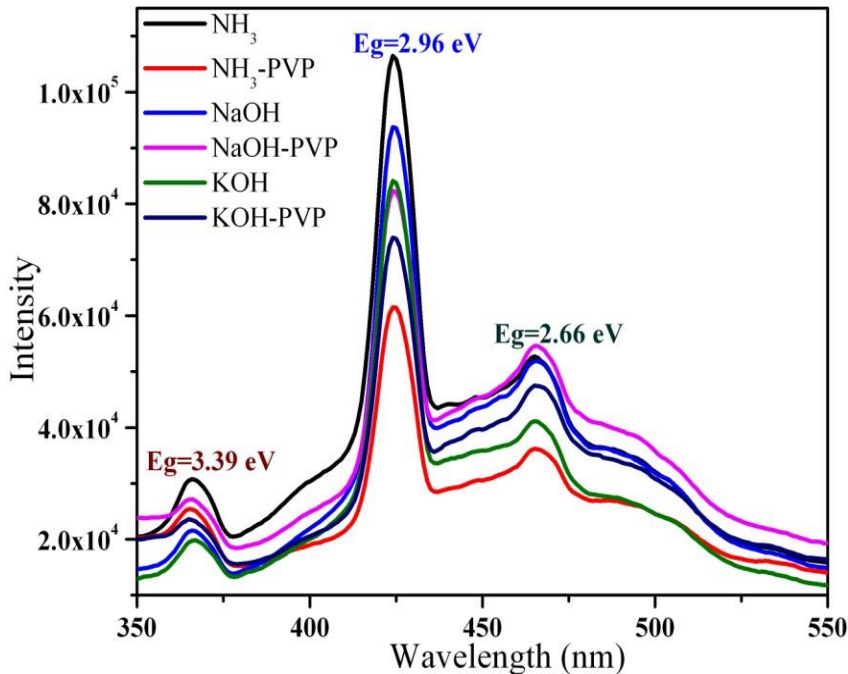


Figure 3. PL spectra of cerium oxide nanoparticles

Conclusion

CeO₂ nanoaggregates are synthesized using various precipitants and dispersant by precipitation method. Cubic fluorite structure of single-phase polycrystalline CeO₂ crystallites is detected from XRD pattern, while the presence of tetravalent Ce⁴⁺ is also evident from the PL spectra. The maximum crystallite size is obtained for the samples prepared from NH₃ while minimum crystallite size is observed for the samples prepared from NH₃-PVP so the dispersant PVP strongly deteriorates the structural properties. Assimilation of PVP strongly increases the transmittance of the samples prepared from KOH precipitant, whereas moderately increases the same prepared from NaOH precipitant but slightly increases the same prepared from NH₃ precipitant. It also firmly affects the growth of O-H, H-O-H and carbonate bands (C=O and COO) whereas slightly affects the growth of C-O stretching vibrations.

References

- [1] E. Kobayashi, Y. Watabe, T. Yamamoto, Y. Yamada, Cerium oxide and hydrogen co-doped indium oxide films for high-efficiency silicon heterojunction solar cells, *Solar Energy Materials & Solar Cells*, 149 (2016) 75-80. <https://doi.org/10.1016/j.solmat.2016.01.005>

- [2] C. Wadia, A.P. Alivisatos, D.M. Kammen, Materials Availability Expands the Opportunity for Large-Scale Photovoltaics Deployment, *Environment Science and Technology*, 43 (2009) 2072-2077. <https://doi.org/10.1021/es8019534>
- [3] N.K. Renuka, A.K. Praveen, C.U. Aniz, Ceria rhombic microplates: Synthesis, characterization and catalytic activity, *Microporous and Mesoporous Materials*, 169 (2013) 35-41. <https://doi.org/10.1016/j.micromeso.2012.10.010>
- [4] S. Thakur, P. Patil, Rapid synthesis of cerium oxide nanoparticles with superior humidity-sensing performance, *Sensors and Actuators B Chemical*, 194 (2014) 260-268. <https://doi.org/10.1016/j.snb.2013.12.067>
- [5] A. Mondal, A. Zachariah, P. Nayak, B.B. Nayak, Synthesis and Room Temperature Photoluminescence of Mesoporous Zirconia with a Tetragonal Nanocrystalline Framework, *Journal of the American Ceramic Society*, 93 (2010) 387-392. <https://doi.org/10.1111/j.1551-2916.2009.03396.x>
- [6] M. Aklalouch, A. Calleja, X. Granados, S. Ricart, V. Boffa, F. Ricci, T. Puig, X. Obradors, Hybrid sol-gel layers containing CeO₂ nanoparticles as UV-protection of plastic lenses for concentrated photovoltaics, *Solar Energy Materials & Solar Cells*, 120 (2014) 175-182. <https://doi.org/10.1016/j.solmat.2013.08.040>
- [7] M.L. Cantu, F.C. Krebs, Hybrid solar cells based on MEH-PPV and thin film semiconductor oxides (TiO₂, Nb₂O₅, ZnO, CeO₂ and CeO₂-TiO₂): Performance improvement during long-time irradiation, *Solar Energy Materials and Solar Cells*, 90 (2006) 2076-2086. <https://doi.org/10.1016/j.solmat.2006.02.007>
- [8] Y.M. Kang, S.H. Kwon, P.K. Song, Study on mechanical and electro-optical properties of ITO/CeO₂ films deposited on PI substrate for flexible organic solar cells, *Current Applied Physics*, 10 (2010) S491-S494. <https://doi.org/10.1016/j.cap.2010.02.039>
- [9] R. Suresh, V. Ponnuswamy, R. Mariappan, Effect of annealing temperature on the microstructural, optical and electrical properties of CeO₂ nanoparticles by chemical precipitation method, *Applied Surface Science*, 273 (2013) 457-464. <https://doi.org/10.1016/j.apsusc.2013.02.062>
- [10] R. Srinivasan, A. Chandrabose, Structural properties of Sm³⁺ doped cerium oxide nanorods synthesized by hydrolysis assisted co-precipitation method, *Materials Letters*, 64 (2010) 1954-1956. <https://doi.org/10.1016/j.matlet.2010.06.023>
- [11] K.M.S. Khalil, L.A. Elkabee, B. Murphy, Preparation and characterization of thermally stable porous ceria aggregates formed via a sol-gel process of ultrasonically dispersed cerium(IV) isopropoxide, *Microporous and Mesoporous Materials*, 78 (2005) 83-89. <https://doi.org/10.1016/j.micromeso.2004.09.019>

- [12] Y. Zhang, Y. Lin, C. Jung, Y. Qin, Formation and Thermal Decomposition of Cerium-Organic Precursor for Nanocrystalline Cerium Oxide Powder Synthesis, *Journal of Dispersion Science and Technology*, 28 (2007) 1053-1058. <https://doi.org/10.1080/01932690701524091>
- [13] D.M. Lyons, K.M. Ryan, M.A. Morris, Preparation of ordered mesoporous ceria with enhanced thermal stability, *Journal of Materials Chemistry*, 12 (2002) 1207-1212. <https://doi.org/10.1039/B104677M>
- [14] C. Chunlin, Y. Shaoyan, L. Zhikai, L. Meiyong, C. Nuofu, Violet/blue photoluminescence from CeO₂ thin film, *Chinese Science Bulletin*, 48 (2003) 1198-1200. <https://doi.org/10.1007/BF03183935>
- [15] C. Sun, H. Li, H. Zhang, Z. Wang, L. Chen, Controlled synthesis of CeO₂ nanorods by a solvothermal method, *Nanotechnology*, 16 (2005) 1454-1463. <https://doi.org/10.1088/0957-4484/16/9/006>

Funding: No funding was received for conducting this study.

Conflict of interest: The Authors have no conflicts of interest to declare that they are relevant to the content of this article.

About The License: © The Author(s) 2021. The text of this article is open access and licensed under a Creative Commons Attribution 4.0 International License